

Effects of Static Axial Strain on the Tensile Properties and Failure Mechanisms of Self-Assembled Collagen Fibers

GEORGE D. PINS, ERIC K. HUANG, DAVID L. CHRISTIANSEN, FREDERICK H. SILVER

Division of Biomaterials, Department of Pathology, University of Medicine and Dentistry of New Jersey, Robert Wood Johnson Medical School, 675 Hoes Lane, Piscataway, New Jersey 08854-5635

Received 23 August 1995; accepted 22 December 1995

ABSTRACT: Collagen fibers form the structural units of connective tissue throughout the body, transmitting force, maintaining shape, and providing a scaffold for cells. Our laboratory has studied collagen self-assembly since the 1970s. In this study, collagen fibers were self-assembled from molecular collagen solutions and then stretched to enhance alignment. Fibers were tested in uniaxial tension to study the mechanical properties and failure mechanisms. Results reported suggest that axial orientation of collagen fibrils can be achieved by stretching uncrosslinked collagen fibers. Stretching by about 30% not only results in decreased diameter and increased tensile strength but also leads to unusual failure mechanisms that inhibit crack propagation across the fiber. It is proposed that stretching serves to generate oriented fibrillar substructure in self-assembled collagen fibers. © 1997 John Wiley & Sons, Inc. *J Appl Polym Sci* **63**: 1429–1440, 1997

Key words: collagen fibers; mechanical properties; fibril structure; tendon/ligament replacement; failure mechanism

INTRODUCTION

Tendons and ligaments are multicomponent, cablelike elements that cyclically transmit force in the absence of permanent length increases.¹ They are composed of structural units termed fascicles containing crimped, aligned, collagen fibril bundles (also termed fibers) that are surrounded by a collagenous sheath. Collagen fibrils in tendon and ligament have been reported to be between 20 and 280 nm in diameter (see Ref. 1 for a summary) and evidence exists for subfibrillar elements with cross-sectional diameters of 3.8 nm.² It has been reported that the ultimate tensile strength of a variety of different types of connective tissue is directly related to the collagen fibril diameters.³ The tensile strengths of wound tissue⁴ and developing chick extensor tendon^{5,6} have

been reported to be directly related to the collagen fibril diameter and length, suggesting that fiber structure may play an important role in dictating the mechanical properties of different tissues.

Our laboratory has studied the self-assembly of type I collagen since the 1970s. This work has led to a better understanding of the assembly process and the manner by which collagen fibrils are built.^{6–9} In addition, self-assembly of collagen fibers has led to development of tissue analogs for producing a number of tissue replacements. One of the devices developed was a replacement for the anterior cruciate ligament (ACL).^{10–16} Major design criteria for an ACL replacement include tensile strength and modulus values similar to those found in normal tissue. Recently, we suggested that the tensile properties of reconstituted collagen fibers are correlated with the degree of fibrillar alignment.¹⁵

The original process for formation of collagen fibers *in vitro* involved the extrusion of collagen

Correspondence to: F. H. Silver

© 1997 John Wiley & Sons, Inc. CCC 0021-8995/97/111429-12

dispersions into a fiber formation buffer and subsequent solvent dehydration, air-drying, and crosslinking.^{14,15} These fibers were reported to have mechanical properties similar to collagen fibers found in rat tail tendons and have a D period characteristic of collagen in tissues.¹² Later, similar fibers were self-assembled from molecular collagen solutions.¹⁵

The purpose of this article was to report results of studies on the structure and mechanical properties of fibers self-assembled from molecular collagen solutions. Results reported below suggest that the mechanical properties of these fibers are enhanced by stretching prior to crosslinking. It is hypothesized based on the appearance of fiber failure surfaces that collagen fibrils present in the outer regions of the fiber are stronger compared to collagen fibrils in the fiber core.

EXPERIMENTAL

Preparation of Soluble Collagen

Acid-soluble collagen was obtained from rat tail tendon as described previously.¹⁷ Collagen fibers were obtained after the skin was removed from the tails of Sprague-Dawley rats. A hemostat was clamped on the thin end of the tail, a tensile force was applied on the clamped end, and the tendon fibers were pulled out of the tendon. The process was repeated until no additional fibers were removed upon subsequent clamping and application of force. Tendon fibers were immersed in 10 mM HCl, pH 2.0 (approximately 10 fibers per 100 mL of solution) for 4 h at RT. The soluble material was separated from the insoluble portion by centrifugation at 30,000*g* at 4°C for 30 min and then sequentially filtered through 0.65 and 0.45 μm filters (Millipore Corp., Bedford, MA). NaCl was subsequently added to the filtrate to a concentration of 0.7*M* and the mixture was allowed to stir for 1 h to precipitate the collagen. The precipitate was collected by centrifugation for 1 h at 30,000*g* at 4°C. The pellet was dissolved in 10 mM HCl, pH 2.0, overnight and dialyzed against 20 mM phosphate buffer, pH 7.4 (disodium hydrogen phosphate), for at least 8 h at room temperature. A second dialysis was then performed against a 20 mM phosphate buffer solution, pH 7.4, for at least 4 h at 4°C. The dialyzate was centrifuged at 30,000*g* for 1 h in the cold and a small amount of HCl, pH 2.0, was added to the pellet. The material was then dialyzed against HCl, pH 2.0, overnight

and the concentration measured using a Gilford spectrophotometer Model 250 (wavelength = 230 nm). Solution concentration was adjusted to 10 mg/mL (1% w/v) and the material was stored in 30 mL syringes prior to fiber extrusion. Based on amino acid analysis and polyacrylamide disc gel electrophoresis, the composition was shown to be consistent with that of type I collagen.¹⁷

Collagen Fiber Production

Collagen fibers were coextruded by connecting a syringe containing the 1% collagen solution to one port of a Micromedics applicator tip (20 ga. × 2 in., Eagan, MN) and a syringe containing phosphate buffer (PBS1) (135 mM NaCl, 30 mM Tris, and 5 mM sodium phosphate dibasic, pH 7.4) to the other port. The two solutions were coextruded by depressing the bar on the applicator tip that pushed the syringe plungers. The solutions were pushed through the two separate metal tubes of the applicator tip until they reached the end of the tip where they joined together. The solutions then were forced through FEP (fluorinated ethylene propylene copolymer) tubing and extruded into a bath of flowing phosphate buffer (PBS1) maintained at 37°C.

Fibers were allowed to self-assemble for 24 h in phosphate buffer (PBS1) and then were immersed in a second phosphate buffer (PBS2) (135 mM NaCl, 30 mM sodium phosphate dibasic, and 10 mM Tris, pH 7.4) for 24 h at 37°C, rinsed in distilled water, and then air-dried under tension as previously described.¹⁵ Fibers were reimmersed in phosphate buffer (PBS2) and allowed to incubate for 1 h at 37°C. The fibers were then extended to various strains using a stretching device shown in Figure 1. Fibers were stretched from 0 to 50% of their original lengths in 5% increments and held at a fixed % stretch for 24 h in phosphate buffer (PBS2) at 37°C. The stretched incubated fibers were then air-dried in the stretching frame, yielding groups of fibers with 0, 10, 15, 20, 25, 30, 40, 45, and 50% stretches. Half of the fibers were crosslinked using severe dehydration for 5 days at 110°C, conditions shown to maximize tensile strength.¹⁸ Collagen fibers from rat tail tendons were prepared as described previously.¹⁵

Mechanical Testing

Load-deformation curves for collagen fibers were determined in tension using an Instron

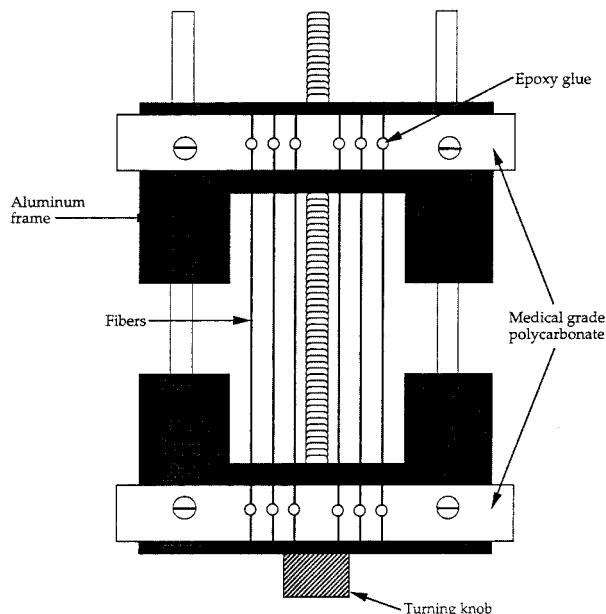


Figure 1 Diagram of device used to stretch self-assembled collagen fibers. Fibers are glued using epoxy to a strip of polycarbonate which are held in place on the frame using screws. The turning knob is twisted and the fibers are stretched to the predetermined final length.

Model 1122 tensiometer (Canton, MA). Using an epoxy adhesive, air-dried fibers from cross-linked and uncrosslinked groups were mounted on paper frames by gluing the ends of the fibers to vertical lines drawn on the frames. Prior to testing, all fibers were immersed in phosphate-buffered saline (PBS) (0.9% (w/v), sodium chloride, and 20 mM disodium hydrogen phosphate) for 60 min. Cross-sectional area was determined by measuring the diameter of the fiber at three places using a Leitz Pol microscope (Rockleigh, NJ) fitted with a calibrated eye piece. It was assumed that the fibers were circular in making cross-sectional area determinations. Fibers were tested using a fixed gauge length of 2.0 cm and a strain rate of 50% per min. The paper frames were clamped into pneumatic serrated grips on the Instron as described elsewhere.¹⁴ Load-extension curves, obtained from the chart recorder, were used to calculate stress-strain behavior, ultimate tensile strength (UTS), and tensile moduli (average slope of the stress-strain curve in linear region). Any fibers which failed at the glue joints were excluded from the experimental data analysis. Statistical comparisons between groups were conducted using an analysis of variance (ANOVA, $P < .05$) and

Fisher's PLSD (Protected Least Significant Difference) analysis ($P < .05$).

The following definitions were used to calculate the mechanical data. The ultimate tensile strength (UTS) was defined as the load at failure divided by the original cross-sectional area; percentage strain at failure was defined as the change in length divided by the original length times 100; and the modulus was defined as the tangent to the stress vs. strain curve in the linear region.

Birefringence Measurements

Semithin ($3 \mu\text{m}$), longitudinal sections of collagen fibers were examined with polarizing optics and monochromatic light to determine the birefringence retardation as described previously.^{6,14} Bundles of collagen fibers, 0.5 cm in length, were tied together with a 6-O prolene suture (Ethicon, Inc., Somerville, NJ) and rehydrated in PBS for 60 min. Fiber bundles were subsequently fixed in Carson's buffered formalin solution (4% formaldehyde in PBS) for 3 h, rinsed in PBS, dehydrated with a graded series of ethanols, and embedded in JB-4 (Polyscience, Warrington, PA). Longitudinal sections of each bundle were cut on a Sorvall MT-2 ultramicrotome with a glass knife and mounted on glass slides. Unstained sections were evaluated using a Leitz 12 Pol microscope (Rockleigh, NJ) fitted with a monochrome filter (wavelength equal to 546 nm), and a Leitz Brack-Kohler $\lambda/10$ calibrated compensator as previously described.⁶

Prior to each birefringence measurement, JB-4 sections were immersed for 90 min in water ($n = 1.333$).⁶ For each bundle of fibers analyzed, six birefringence measurements were made on randomly selected regions. Statistical analyses were conducted as described above for mechanical testing.

Scanning Electron Microscopy (SEM)

Collagen fibers that were pulled to failure in mechanical tests were processed for SEM by immersion in modified Karnovsky's fixative for 24 h. Fibers were then rinsed several times in cacodylate buffer and dehydrated through a graded series of ethanol solutions of increasing concentrations. After ethanol dehydration, specimens were subjected to vacuum sublimation in Peldri (Ted Pella Inc., Redding CA), sputter-coated with gold, and

observed in an Amray SEM Model 1400 operated at 20 kV.

RESULTS

Mechanical Testing

The purpose of this study was to determine whether improved tensile strengths could be accomplished by stretching extruded collagen fibers prior to final crosslinking. This was tested by placing dry extruded collagen fibers in a stretching device, rehydrating them, and then stretching them to a set level followed by air drying. Typical stress–strain curves for uncrosslinked and crosslinked collagen fibers are compared to fibers from rat tail tendons in Figure 2. Results of all mechanical tests are compiled in Table I.

The diameter of rehydrated stretched fibers was found to decrease from about 327 μm at 0% stretch to about 146 μm at about 35% stretch (Fig. 3). The wet diameters of fibers stretched 0, 10, 15, and 20% were significantly different from the diameters of fibers stretched in excess of 20%. Fibers stretched 25 and 30% had wet diameters that were larger than fibers stretched greater than 30%. Fibers stretched 35, 40, 45, and 50% had similar diameters.

The load at failure increased from about 7.55 g at 0% stretch to about 14 g at 30% and then fell to 12.3 g at 50% stretch (Fig. 4). The load at 30% stretch was significantly greater than all the other loads at failure. Percentage strain at failure decreased from about 68% at 0% stretch to about 25% at 35% stretch (Fig. 5). Strain at 35% stretch was significantly lower than that at 45% stretch and it was equal to that at 40 and 50%.

Modulus and UTS values also increased with percentage stretch (Figs. 6 and 7). Modulus increased from 1.82 MPa at 0% stretch to 45 MPa at 50% stretch (Fig. 6). Although the modulus decreased between 35 and 40% stretch, the value at 50% was significantly greater than that at any other % stretch. UTS values increased from 0.91 MPa at 0% stretch to 6.64 MPa at 35% stretch (Fig. 7). The value at 35% was not significantly different from values at 40% and greater; however, it was greater than values at stretches of 25% and less.

For crosslinked fibers, the wet fiber diameter decreased from 93 μm at 0% stretch to 80 μm at 50% stretch (Fig. 3). Fiber diameters at 20 and

40% were greater than diameters observed at 50% stretch. Load at failure increased from about 28.9 g at 0% stretch to 42.7 g at 30% stretch (Fig. 4). The load at failure at 0% stretch was significantly less than the values at 20, 30, and 40% stretch, but there was no significant difference between the loads for the fibers stretched between 10 and 50%.

The strain at failure varied from 16.9% for 0% stretch to 12.3% at 30% stretch (Fig. 5). Strains to failure at 40 and 50% stretch were not significantly different from that at 30%. Modulus values varied from 383 MPa at 0% stretch to 726 MPa at 30% stretch (Fig. 6). Values at 40 and 50% stretch were not significantly greater than those at 30%. UTS values ranged from 46.8 MPa at 0% stretch to 71.5 MPa at 30% stretch (Fig. 7). Values at 40 and 50% stretch were not significantly different from the value at 30%.

SEM

Scanning electron microscopic evaluations of the failure surfaces of uncrosslinked collagen fibers (Fig. 8) showed that the outer surface of the fiber appeared to have deformed more than the inner core, resulting in greater relaxation and retraction of the outer portion relative to the inner portion. Tensile and torsional forces created in the fiber due to axial tension caused necking (50% stretch) as diagrammed in Figure 9 and twisting [see Fig. 8(A)]. In contrast, the surface of crosslinked fibers stretched in excess of 30% showed a characteristic “splinter” failure [Fig. 8(C) and 9]. Initiation of failure occurred by a crack propagating a distance across the fiber axis at which point it propagated parallel to the fiber axis until failure occurred. It is not possible to conclude from stress–strain and SEM studies whether the distance that the crack initially propagated across the fiber axis was large or small. Since the stress was not typically observed to fall prior to catastrophic fiber failure, it is likely that the initial crack only propagated a short distance across the fiber axis.

SEM observations on rat tail tendon fibers indicated that fibers failed by fibrillar slippage (Fig. 8). The morphology of the failed fiber ends was similar to the ends of the uncrosslinked, stretched, self-assembled collagen fibers.

Birefringence Retardation

Birefringence retardation measurements were made on semithin (3 μm) sections of un-

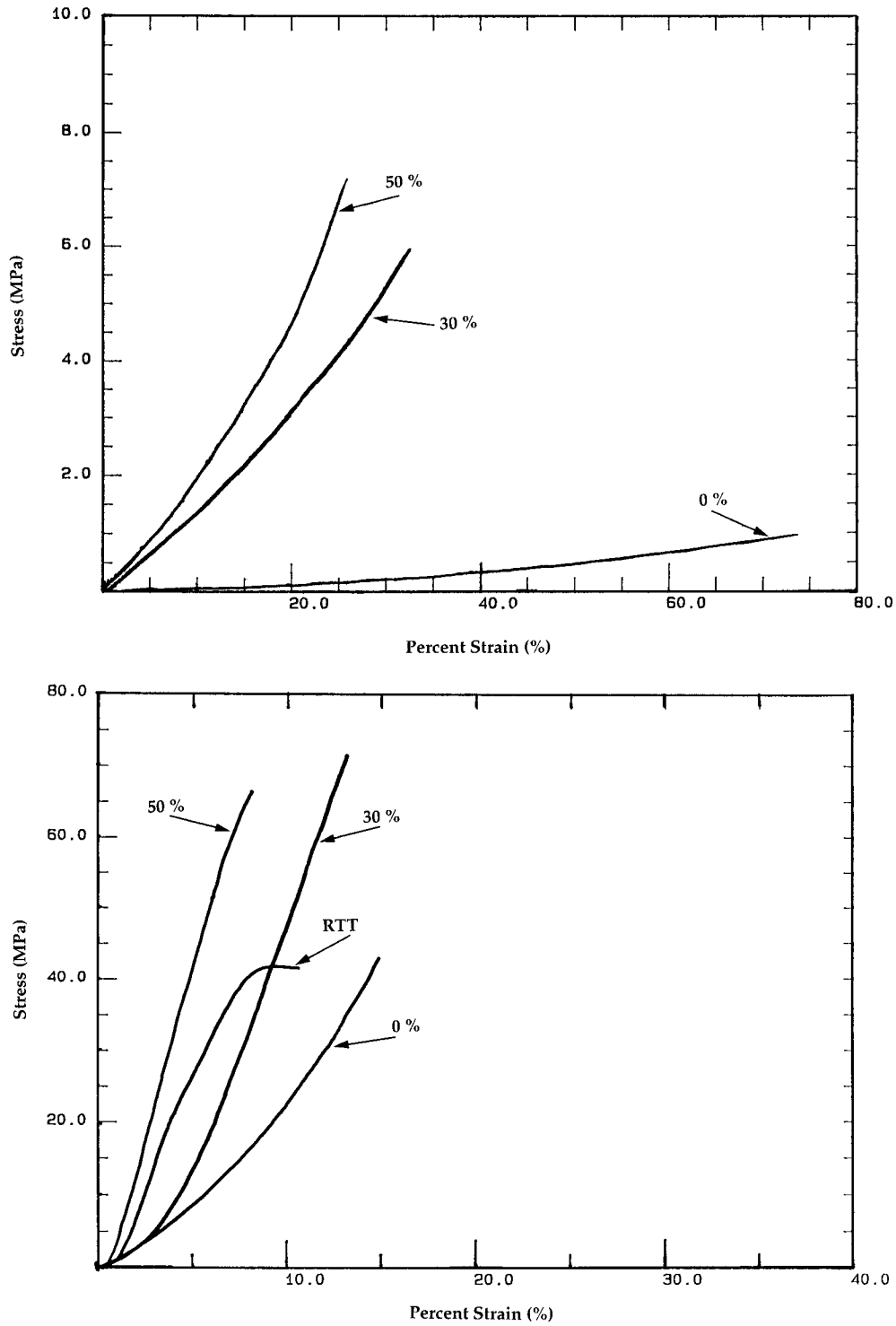


Figure 2 Typical stress vs. strain curves for (a) uncrosslinked fibers stretched 0, 30, and 50% and (b) crosslinked self-assembled collagen fibers stretched 0, 30, and 50% and for rat tail tendon (RTT) fibers. The fibers were tested in uniaxial tension at a strain rate of 50% per min.

Table I Mechanical Properties of Stretched Collagen Fibers

% Stretch (<i>n</i>)	UTS (MPa)	Strain at Failure (%)	Modulus (MPa)		Wet Diameter (μm)	Load at Failure (g)
0- <i>U</i>	0.908 \pm 0.208	67.97 \pm 6.874	1.819 \pm 0.344		327.1 \pm 33.68	7.550 \pm 0.883
10- <i>U</i> (24)	2.009 \pm 1.198	45.14 \pm 8.968	5.701 \pm 2.475		253.3 \pm 33.65	9.611 \pm 3.626
15- <i>U</i> (23)	2.911 \pm 0.822	39.71 \pm 7.741	9.255 \pm 1.654		213.6 \pm 17.58	10.92 \pm 4.079
20- <i>U</i> (24)	3.924 \pm 2.093	36.52 \pm 6.418	12.88 \pm 6.482		199.5 \pm 32.79	11.08 \pm 3.566
25- <i>U</i> (24)	5.004 \pm 0.977	32.00 \pm 6.689	20.32 \pm 9.147		168.5 \pm 24.91	11.22 \pm 2.460
30- <i>U</i> (23)	5.943 \pm 1.277	32.47 \pm 4.761	20.78 \pm 4.336		173.2 \pm 13.09	14.00 \pm 2.418
35- <i>U</i> (24)	6.644 \pm 1.654	24.83 \pm 4.538	35.03 \pm 14.35		146.2 \pm 14.01	11.14 \pm 2.098
40- <i>U</i> (23)	6.323 \pm 1.183	26.82 \pm 4.795	27.25 \pm 9.708		141.1 \pm 11.96	9.949 \pm 1.452
45- <i>U</i> (20)	7.363 \pm 1.789	29.73 \pm 7.149	37.59 \pm 18.00		147.7 \pm 22.77	12.41 \pm 2.002
50- <i>U</i> (20)	7.217 \pm 1.260	24.12 \pm 5.674	45.97 \pm 19.92		147.2 \pm 14.11	12.32 \pm 1.683
0- <i>X</i> (24)	46.81 \pm 17.11	15.59 \pm 2.66	383.0 \pm 111.7		94.00 \pm 11.54	31.73 \pm 9.071
10- <i>X</i> (24)	51.62 \pm 17.04	15.50 \pm 2.61	428.8 \pm 110.8		95.63 \pm 10.27	37.01 \pm 11.43
20- <i>X</i> (24)	59.25 \pm 13.33	13.93 \pm 2.10	544.2 \pm 91.55		91.88 \pm 6.867	40.56 \pm 11.87
30- <i>X</i> (24)	71.49 \pm 18.26	12.34 \pm 1.75	725.7 \pm 120.2		86.13 \pm 11.05	42.71 \pm 14.74
40- <i>X</i> (24)	63.61 \pm 15.89	11.21 \pm 2.04	729.2 \pm 119.4		88.04 \pm 15.31	38.90 \pm 11.40
50- <i>X</i> (23)	68.82 \pm 15.75	11.65 \pm 2.49	766.5 \pm 111.0		80.27 \pm 9.794	36.21 \pm 11.95

U = uncrosslinked fibers; *X* = crosslinked fibers.

crosslinked and crosslinked collagen fibers. The results of these experiments are summarized in Figure 10. Form birefringence analyses, which measure the degree of ordered aggregation of fibrils within a fiber, were made on sections of fibers by immersing them in water ($n = 1.333$). Measurements made on uncrosslinked collagen fibers showed that there was no significant statistical variation in form birefringence when fibers were stretched between 0 and 50% of their initial length, but

fibers that were stretched at least 20% had birefringence values comparable to rat tail tendon fiber (Fig. 10). Analyses of measurements on crosslinked collagen fibers showed that fibers stretched at least 30% had form birefringence values comparable to native rat tail tendon fibers and significantly greater than fibers stretched up to 20% (Fig. 10). Additionally, fiber stretched 30% exhibited form birefringence values which were significantly higher than comparable fiber stretched 40%.

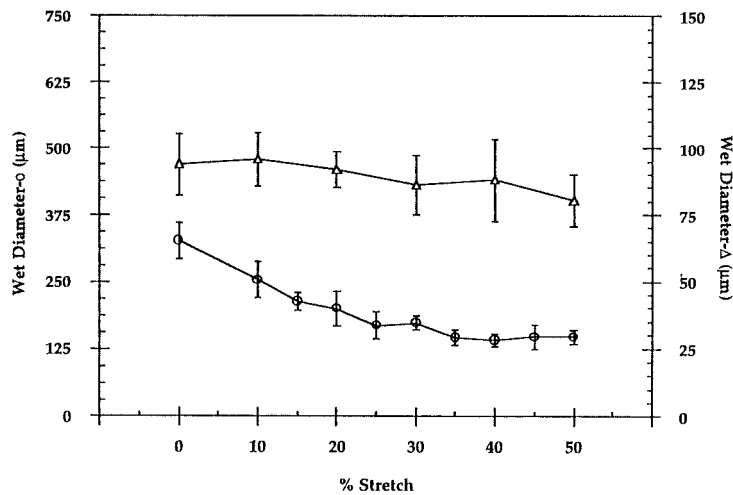


Figure 3 Wet collagen fiber diameters for (\circ) uncrosslinked and (Δ) crosslinked collagen fibers vs. % stretch.

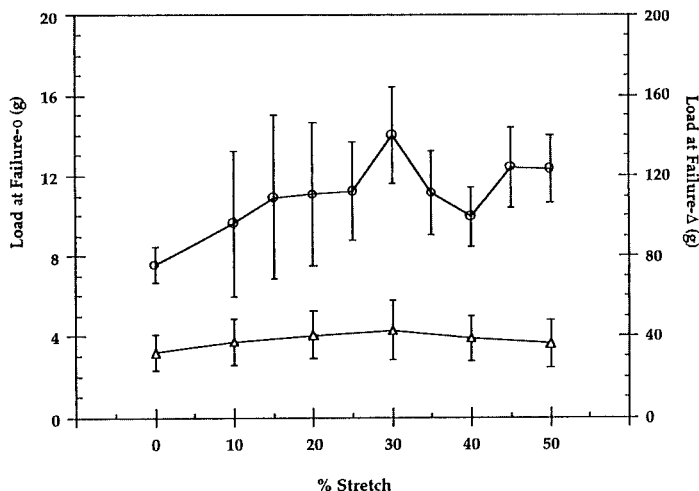


Figure 4 Load at failure vs. % stretch for (○) uncrosslinked and (△) crosslinked collagen fibers.

DISCUSSION

Collagen fibers form the structural framework of all tissues, giving shape to masses of cells, providing resistance to mechanical trauma, and transmitting forces in the musculoskeletal system. Although there are a number of collagen types found in the fibrous components of connective tissue, type I collagen is responsible for force transmission in tendons and ligaments. It is well documented that the ultimate tensile strength of collagen fibers in tissues is directly related to the fibril³ and fiber^{4,6} diameters as well as to fibril bundle length.⁶

We have developed a model system for self-as-

sembly of collagen fibers from collagen molecular solutions. The relationship between hierarchical structure and mechanical properties of collagen fibers can be explored using this model system. In addition, these fibers are also suitable for constructing tissue replacements that mimic the structures of biological tissues.

The results of this study suggest that that the mechanical properties and failure modes of self-assembled collagen fibers are very sensitive to the degree of fiber stretch that is applied prior to the fiber being crosslinked. Fiber diameter decreased with increasing degree of stretch and load to failure increased at 30% stretch. These changes led to an increased value of the UTS. Based on the

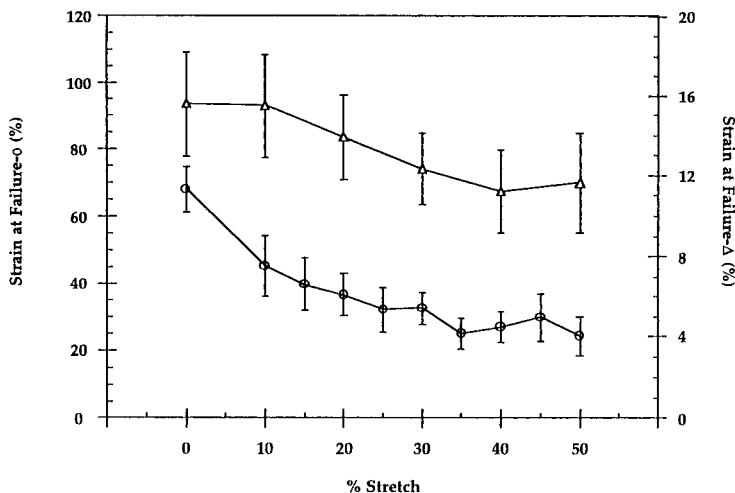


Figure 5 Strain at failure vs. % stretch for (○) uncrosslinked and (△) crosslinked collagen fibers.

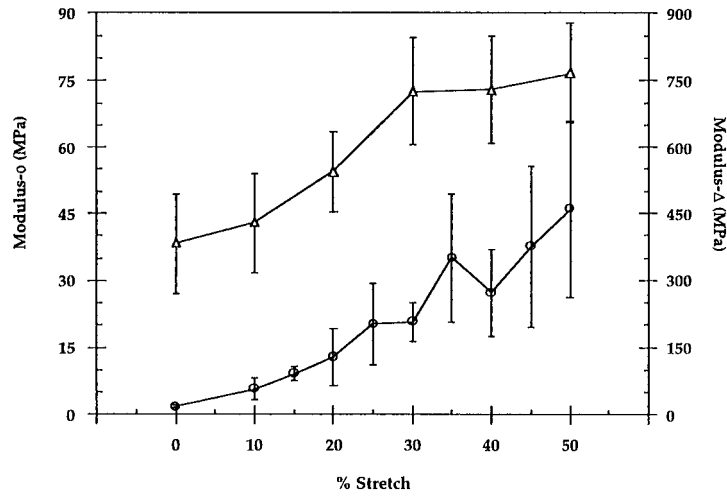


Figure 6 Modulus in linear region vs. % stretch for (○) uncrosslinked and (△) crosslinked collagen fibers.

observed failure modes for both uncrosslinked and crosslinked fibers, we hypothesize that self-assembly followed by axially induced strain may lead to a fiber with a nonuniform cross section. Analysis of the failure surfaces led us to propose that stretching generated an outer surface with oriented collagen fibrils that appeared to be more extensible and perhaps stronger than the inner core. This would explain the necking observed with stretched uncrosslinked fibers and the splintering effect seen with stretched crosslinked fibers. However, the observed failure pattern may also be explained if the fibrils on the outer surface are more highly crosslinked than those in the center.

The observation that crack propagation was

both perpendicular as well as parallel to the fiber axis suggests that high tensile strength may be, in part, produced by the presence of structural units aligned along the fiber axis. This is consistent with a model that has an outer layer of axially aligned collagen fibrils surrounding a less oriented inner core of fibrils or an outer layer that is more highly crosslinked. Based only on SEM and mechanical test results, it is not possible to conclude which of these models explains the observed failure behavior. However, it is reasonable to suggest that subfibrillar subunits may be generated by postextrusion incubation and stretching of collagen fibers self-assembled from molecular solutions in PBS.

The observation that the degree of fibrillar ori-

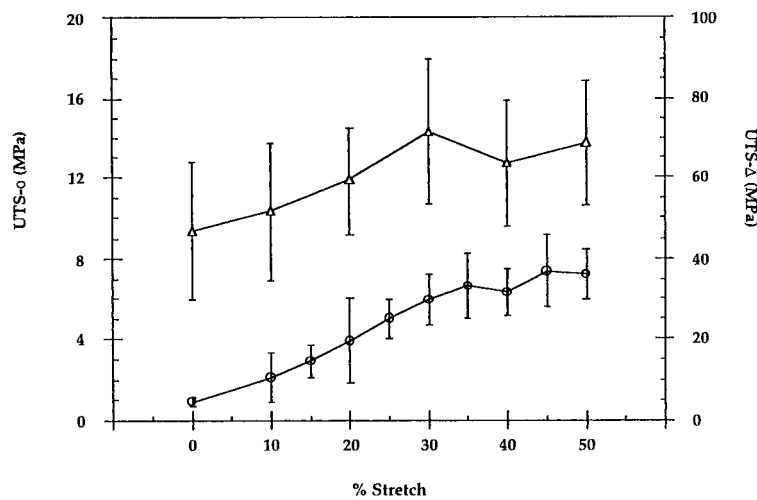


Figure 7 UTS vs. % stretch for (○) uncrosslinked and (△) crosslinked collagen fibers.

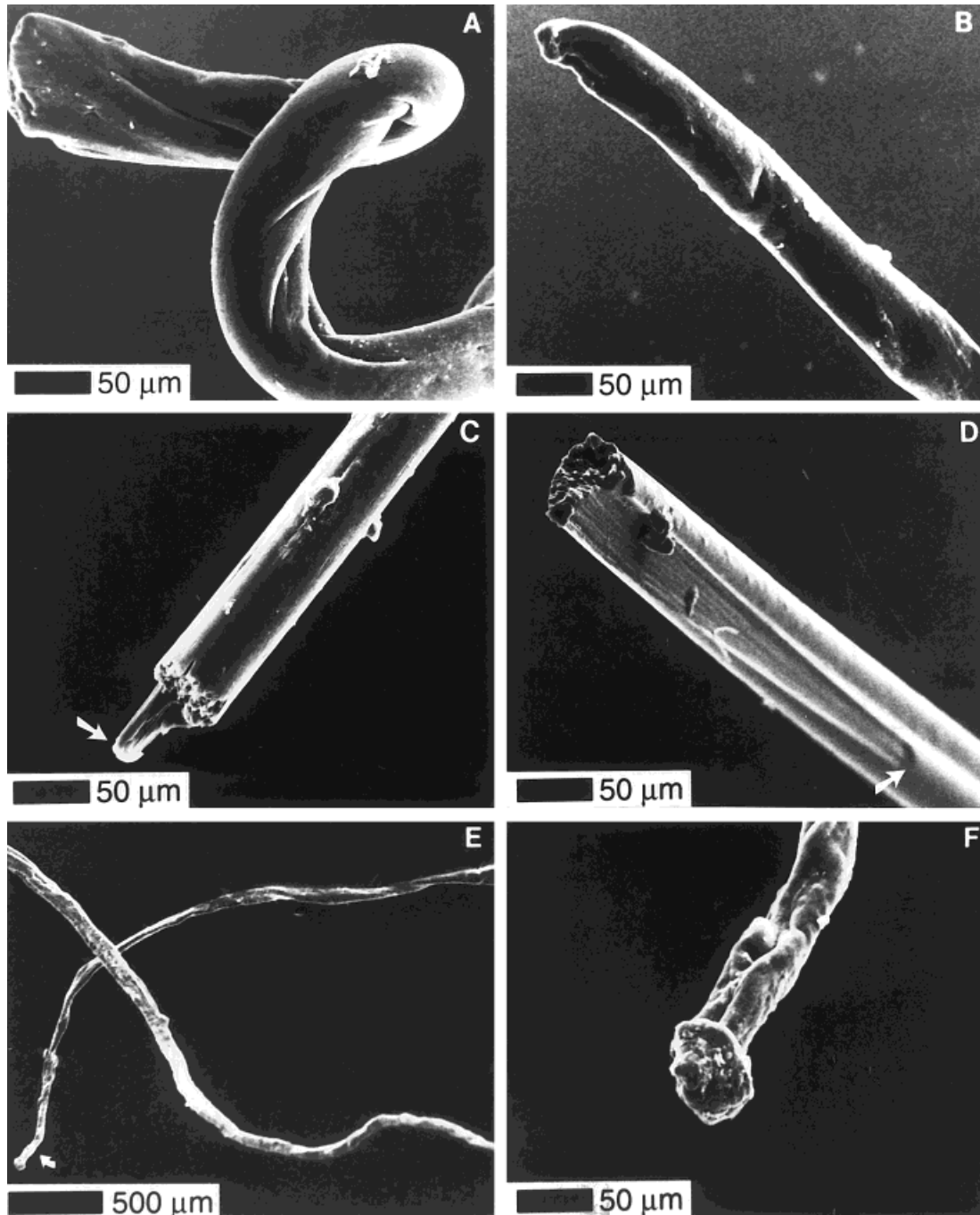
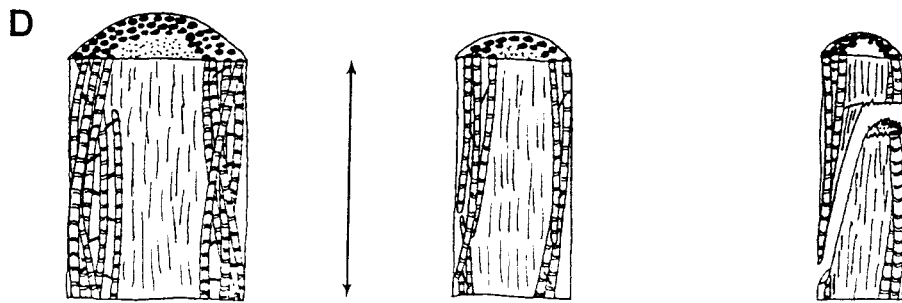
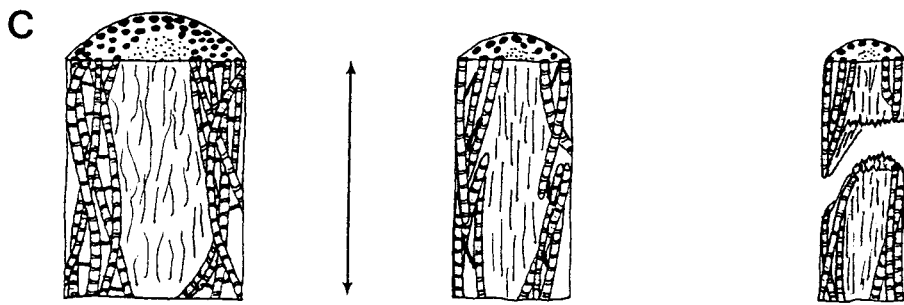
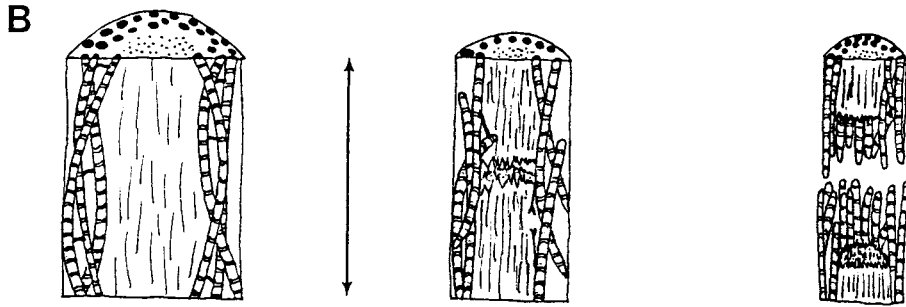
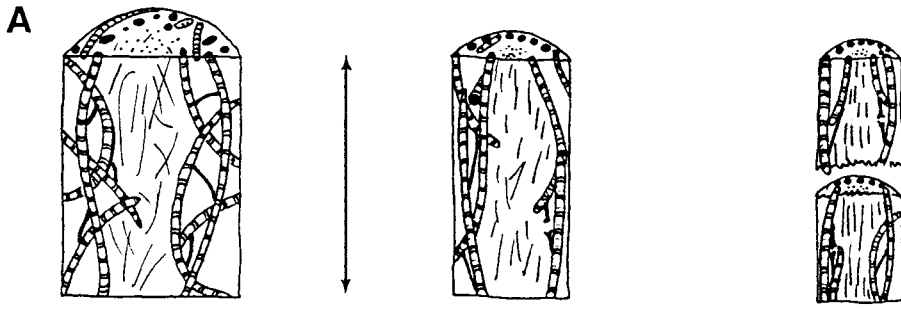


Figure 8 SEMs of failure surfaces of (A) uncrosslinked unstretched, (B) uncrosslinked stretched 50%, (C) crosslinked stretched 30%, and (D) 50% and rat tail tendon fiber pulled to failure at (E) low and (F) high magnification. The arrow in (E) is magnified in (F).

entation was similar for uncrosslinked collagen fibers (stretched 20% or more or crosslinked collagen fibers stretched in excess of 30%) to the orientation of collagen in rat tail tendon fibers suggests that axially induced strain may result in in-

creased collagen fibril orientation based on birefringence values. Increased collagen fibril orientation leads to increased ultimate tensile strength and modulus while reducing the strain at failure. Since birefringence data are averaged across the



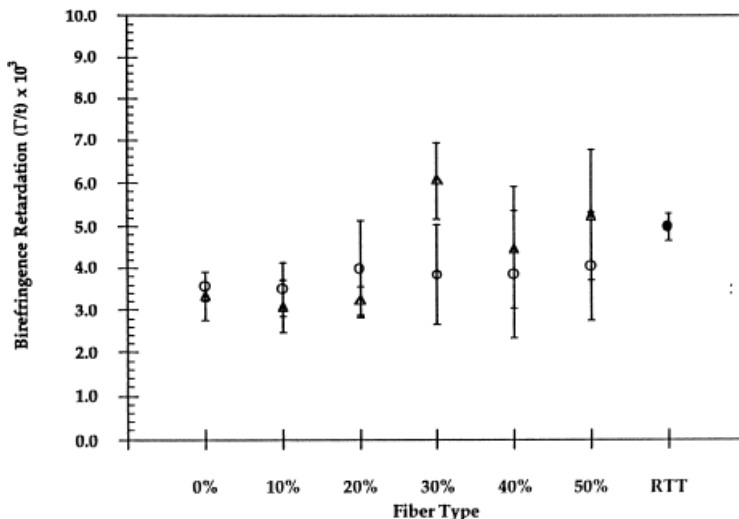


Figure 10 Birefringence retardation (Γ) per unit fiber thickness (t) for collagen fibers stretched between 0 and 50% and rat tail tendon fibers. The open triangles represent points for crosslinked fibers while the closed circles represent points for uncrosslinked fibers.

fiber diameter, these results are consistent with the hypothesis that the outer portion of stretched fibers contain axially aligned collagen fibrils. However, it does not rule out other possible explanations.

A great deal of basic research has been devoted to understanding the substructure of collagen fibers in a variety of tissues including tendons. Crystalline units within collagen fibrils have been observed based on TEM observations and hypothesized based on optical diffraction conducted on negatives of fibril cross sections.² However, the evidence for a microfibril that is a structural unit from which the fibril is constructed is still inconclusive. From a biomechanical prospective, the

presence of discrete subfibrillar units in aligned connective tissue would serve to inhibit crack propagation across collagen fibrils when tissues are loaded in tension along the axis. It is possible that the presence of microfibrillar subunits that are aligned by stretching self-assembled collagen fibers can explain the failure mechanisms observed in this study.

In summary, using a model collagen self-assembly system, we have shown that axial orientation of collagen fibrils can be achieved by stretching collagen fibers in the uncrosslinked state. Stretching collagen fibers by about 30% prior to crosslinking not only increases the tensile strength but also creates unusual failure mecha-

Figure 9 Diagram illustrating collagen fibers (left) prior to, (center) during, and (right) after mechanical loading. Fibers depicted include (A) unstretched uncrosslinked, (B) stretched uncrosslinked, (C) 30% stretched crosslinked, and (D) 50% stretched crosslinked collagen fibers. In (A), the unstretched uncrosslinked fiber undergoes outer fibril alignment during tensile testing prior to failure. On failure, the retraction of the outer aligned fibrils causes the failure surface to be convex. Fiber stretching prior to mechanical testing increases the difference between the fibril alignment of the outer and inner portions. On mechanical testing, failure occurs within the inner core and the outer aligned layer collapses over the region where the core has contracted back. This leaves the end appearing drawn out (B). Fibers stretched by 30%, crosslinked, and tested in tension have the aligned outer portion found in uncrosslinked fibers which is strengthened by crosslinking. The inner core again fails and the crack travels perpendicular to the fiber axis until it is stopped by the collagen fibrils aligned parallel to the axis (C). This causes the fiber to splinter as the crack leads to failure. When the fiber is stretched 50% prior to crosslinking the length of the splinter increases because the outer fibrils are more highly aligned (D).

nisms that inhibit crack propagation transversely across the fiber. Based on these observations, it is proposed that stretching may serve to generate such fibrillar axial alignment; however, further studies are necessary to test this hypothesis.

REFERENCES

1. F. H. Silver, Y. P. Kato, M. Ohno, and A. J. Wasserman, *J. Long-Term Effects Med. Implants*, **2**, 165–198 (1992).
2. D. J. S. Hulmes, J.-C. Jesior, A. Miller, C. Berthet-Columinas, and C. Wolff, *Proc. Natl. Acad. Sci. U.S.A.*, **78**, 3567–3571 (1981).
3. D. A. D. Parry, G. R. G. Barnes, and A. S. Craig, *Proc. R. Soc. Lond. B.*, **203**, 305–321 (1978).
4. C. J. Doillon, M. G. Dunn, and F. H. Silver, *J. Biomech. Eng.*, **110**, 352–356 (1988).
5. D. J. McBride, R. A. Hahn, and F. H. Silver, *Int. J. Biol. Macromol.*, **7**, 71–76 (1985).
6. D. J. McBride, R. L. Trelstad, and F. H. Silver, *Int. J. Biol. Macromol.*, **10**, 194–200 (1988).
7. F. H. Silver, K. H. Langley, and R. L. Trelstad, *Biopolymers*, **18**, 2523–2535 (1979).
8. J. Brokaw, C. J. Doillon, R. A. Hahn, D. E. Birk, R. A. Berg, and F. H. Silver, *Int. J. Biol. Macromol.*, **7**, 135–140 (1985).
9. S. Farber, A. Garg, D. E. Birk, and F. H. Silver, *Int. J. Biol. Macromol.*, **8**, 37–42 (1986).
10. J. D. Goldstein, A. J. Tria, J. P. Zawadsky, Y. P. Kato, D. Christiansen, and F. H. Silver, *J. Bone J. Surg.*, **71-A**, 1183–1191 (1989).
11. Y. P. Kato, M. G. Dunn, J. P. Zawadsky, A. J. Tria, and F. H. Silver, *J. Bone J. Surg.*, **73-A**, 561–574 (1991).
12. D. Christiansen, G. Pins, M. C. Wang, M. G. Dunn, and F. H. Silver, *Mater. Res. Symp. Proceed.*, **252**, 151–158 (1992).
13. M. G. Dunn, A. J. Tria, Y. P. Kato, J. R. Bechler, R. S. Ochner, J. P. Zawadsky, and F. H. Silver, *Am. J. Sports Med.*, **20**, 507–515 (1992).
14. Y. P. Kato, D. L. Christiansen, R. A. Hahn, S.-J. Shieh, J. Goldstein, and F. H. Silver, *Biomaterials*, **10**, 38–42 (1989).
15. G. D. Pins and F. H. Silver, *Mater. Sci. Eng. Biomim. Mater. Sensors Syst.*, to appear.
16. F. H. Silver and Y. P. Kato, U.S. Pat. 5,171,273 (1992).
17. F. H. Silver and R. L. Trelstad, *J. Biol. Chem.*, **255**, 9427–9433 (1980).
18. M.-C. Wang, G. D. Pins, and F. H. Silver, *Biomaterials*, **15**, 507–512 (1994).